Desalination and Water Treatment
www.deswater.com
doi: 10.5004/dwt.2020.25527

Direct solar desalination using nano/micro-porous polymeric membrane via thin film evaporation

Mona Bahman, Arwa AlShareif, Faisal AlMarzooqi, Ibrahim Mustafa

ABSTRACT

Thin film evaporation from nanoporous membranes is a promising thermal desalination approach because it utilizes the passive capillary pumping of liquid to the evaporating interface and allows for high heat transfer rates due to the large evaporating area in addition to the capillary pumping driving force. In this study, solar energy was used as a heat source to evaporate seawater through in-house fabricated polyvinylidene fluoride (PVDF) nano/micro-porous membranes incorporated with nanoparticles. Compromising between the available area for evaporation via changing pore size and the available material for conductive transfer of heat to the liquid thin film is complicated and require a deep study experimentally and theoretically. The objectives of this study are to investigate the pore size effect and thermal conductivity on the vapor flux by fabricating fumed silica and carbon nanotube membranes. The fabricated membranes were characterized by scanning electron microscopy, contact angle analyzer (CA), capillary flow porometry and porosity to further understand the observed thin film evaporation effects. The preliminary results showed that CNT is an effective nanoparticle to obtain higher vapor flux (18.48903 g/min m^{-2}) in thin film evaporation that incorporated with solar simulator this is due to good ability of CNT to absorb light and converted to thermal energy. It is recommended to investigate more membranes with deep analysis to achieve the paper objective.

Keywords: Thin film evaporation; Nanoparticles; Carbon nanotube; Fumed silica; Pore size; Thermal conductivity

1. Introduction

Water is a very valuable element for nature, human life and global economy. It provides a sustainable high-quality for agriculture, industry, recreation, energy production, and domestic consumption (Gewin 2005). About 97% from the total mass of water on the world is salty and 3% is freshwater. However, most of the 3% of freshwater is trapped in glaciers and ice caps making it difficult to reach (Gleick 1996). So, in this world we are suffering from freshwater scarcity which is a critical problem worrying people. Especially with the increase in population number, demand for water is increased in addition to the rise in water pollution. Because of that the need of alternative resources of freshwater is a must, therefore many technologies have existed to solve this problem.

One of the newest technology is using thin film evaporation combined with solar simulation to generate steam (Peng et al. 2018). As solar energy is renewable and environment friendly, it will be utilized as source of heat to evaporate water. Beside the solar energy many studies have been made to enhance the evaporation rate by incorporation of nanoparticles in thin film evaporation membrane (Plawsky et al. 2014). Seeding membranes with nanoparticles will increase the surface area and will enhance the thermal properties of the membrane (Ni 2014). Recently, Neumann et al. 2012 was able to generate steam in bulk water with Au nanoparticles (NPs) with the power of 10^3 kWm^{-2}. Carbon nanotubes [7] and fumed silica nanoparticles (Suzuki et al. 2014) were used in this study.

Compromising between the available area for evaporation via changing pore size and the available material for conductive transfer of heat to the liquid thin film is complicated. Since more porous membrane increases the evaporation surface area and at the same time this leads to having less conductive material for heat transfer which at the end will reduce the evaporation rate. The aim of this study is to develop an efficient nonporous membrane based water desalination system that can eventually be incorporated into a solar radiation. This paper will focus on, investigating the pore size and meniscus shape effect on the vapor flux by fabricating flat sheet CNT membranes mixed with PVDF. In addition, examining the thermal conductivity effect on

Presented at the 13th Gulf Water Conference – Water in the GCC: Challenges and Innovative Solutions. 12–14 March 2019, Kuwait

the vapor flux by changing the concentration of fumed silica in the PVDF polymeric solution. Therefore, it is best to choose the favorable nanoparticle for solar absorption in thin film evaporation with higher efficiency.

2. Methodology

2.1. Materials

PVDF (Kynar 741) is the polymer used in fabrication and it was obtained from Arkema. PVDF has favorable properties as a material for fabricating porous membranes via the phase inversion technique. Ethanol and dimethylacetamide (DMAc) supplied by Alfa Aesar (>99.5% purity) were used as the solvent for PVDF. The functionalized carbon nanotube with PEG and modified fumed silica with a surface area of 125 m^2/g was used as the additive to the membrane sheet.

2.2. Membrane preparation

2.2.1. CNT membrane

PVDF and CNT were ground in ethanol and then added to 50% solution of ethanol and DI water, the solution was sonicated at 40 W of power for 15 min. The prepared solution was casted on copper sheet using doctor blade with thickness of 5 mm. Two different drying methods used in CNT fabrication (oven and freezer) in order to manipulate the pore size of the membrane.

2.2.2. FS membrane

Phase inversion technique was followed to fabricate FS membrane, in which PVDF, FS, DMAc were blended for 8 h using a magnetic stirrer and sonicated for 10 min to have homogeneous solution and later it is kept for 24 h for degassing. The prepared solution was casted using doctor blade with thickness of 500 μm on a non-woven support (Novatexx 2471, donated by Freudenberg-Filter, Germany) at 60% relative humidity. The casted membrane was immersed in a coagulation bath containing deionized water (Mavukkandy et al. 2017).

2.3. Membrane characterization

The microstructure of the membrane surface was observed using scanning electron microscopy (SEM, Quanta-250, FEI, Hillsboro, OR, USA). Samples were coated with gold and palladium at 50 Å thickness in order to create conductive surfaces. The mean pore size and pore size distribution were measured using a capillary flow porometer (CFP, Porous Materials Inc., Ithaca, NY, USA) using Galwick as the wetting liquid. A gravimetric method was used in order to calculate volume porosity using Galwick®. To test the hydrophobicity of the membrane, the contact angle on the membrane surface of DI water was measured using the sessile drop method with a contact angle goniometer (KrüssDSA 10 Mk2, Hamburg, Germany). To enhance the data accuracy, at least six drops at different location of the sample were taken and their readings were averaged. Other studies such as thermal analysis and UV absorption are in the progress.

2.4. Thin film evaporation experiment

Thin film evaporation experiments were carried out under controlled conditions using a lab-scale setup. The experimental device was designed (Fig. 1) for nonporous membrane to achieve high evaporation flux over a large area using solar simulator as a source of heat.

The feed liquid was 35 g/L NaCl solution and DI water which passes to the supported membrane structure at room temperature through the connected pipe and circulated at a constant flow rate of 15 mL/min. Due to capillary effect of nonporous membrane, the water flowing through the membrane pores and evaporating from the membrane surface by absorbing heat from the solar simulator. The water passes throughout the structure and circulated back to the system. The mass of the water was measured at steady-state condition for 6 h in order to measure the evaporation flux due to the mass change over the period. The electrical conductivity was measured at the beginning and at the end of the running experiment for each sample.

3. Result and discussion

3.1. Effect of mass change of FS on evaporation flux

Fig. 2 shows how the mass changed of the vapor with source of heat and without it for each membrane. Starting with FS membranes, the result shows that at time = 4 h the change of mass are about 2.5 g for FS-3 and FS-4, while it is slightly increased in FS-5 reaching 3 g at $t = 4$ h as shown in Figs. 2b, d and f, respectively. The calculated evaporation flux shows the same trend as well, since FS-3 and FS-4 have almost the same evaporation flux 7.89525 and 7.929286 g/min m^{-2}, respectively, while FS-5 membrane provides better evaporation flux 9.334505 g/min m^{-2} (Fig. 3).

3.1.1. Morphology

The physical characteristics were examined to understand the membrane mechanism. Fig. 4 shows the morphologies of FS-3, FS-4 and FS-5, which all have the same structure at different magnification. This is because of only a slight change of added fumed silica in each membrane while other parameters are constant.

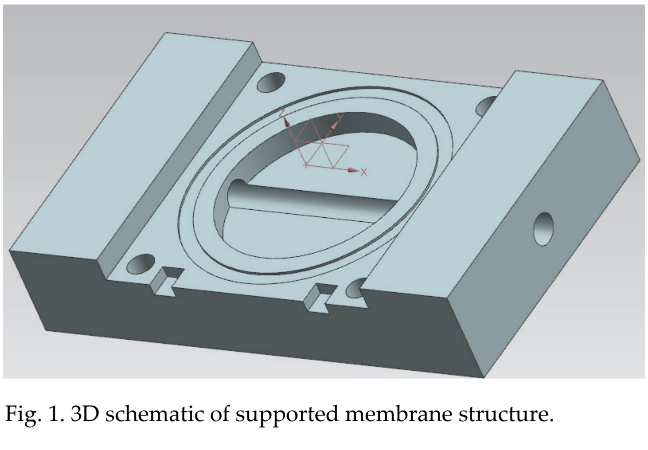

Fig. 1. 3D schematic of supported membrane structure.

3.1.2. Porosity and wettability

The listed result in Table 3 shows the different porosity % and mean pore size among FS-3, FS-4 and FS-5, but FS-3 and FS-4 have close result. However all FS membrane have CA in range of 75°, see Fig. 5.

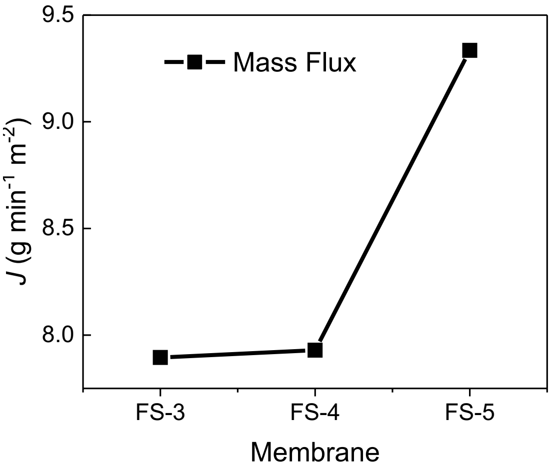

Fig. 2. Evaporation flux of FS membranes

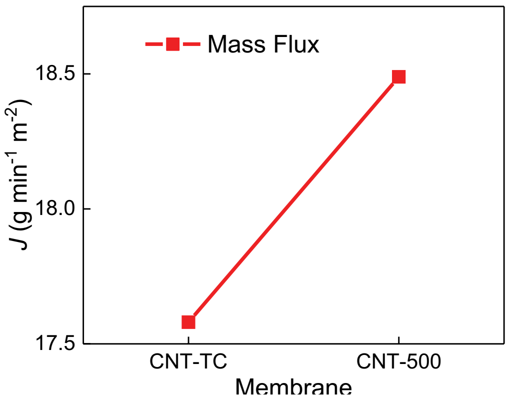

Fig. 3. Evaporation flux of FS membranes.

Table 1
CNT membrane preparation parameters and membrane thickness

Membrane Code	PVDF mg	CNT mg	Drying method	Thickness µm
CNT-TC	400 mg	400 mg	Oven at 120°C	200
CNT-500	400 mg	400 mg	Freezer	203
CNT-1000	400 mg	400 mg	Freezer	190

Table 2
FS Membrane preparation parameters and membrane thickness

Membrane code	PVDF wt%	Fumed silica wt%	DMAc wt%	Thickness µm
FS-3	15	3	82	410
FS-4	15	4	81	400
FS-5	15	5	80	530

3.1.3. Thermal analysis

The study of thermal conductivity was one main objectives of this paper. It's expected that, the evaporation flux will increase as the thermal conductivity increase. This study is still in progress and more samples with various mass of FS will be fabricated to achieve the objective.

3.2. Effect of CNT membrane on evaporation flux

Comparing the CNT result with FS membranes, the mass changed during the thin film evaporation experiment was higher in CNT membrane, at t = 4 hr the evaporated mass exceed 4 g in both CNT-TC and CNT-500 membranes. This is because of the better light absorbance in black membrane as shown in Fig. 2, since the temperature change in CNT membrane were higher than FS membranes. The evaporation flux was 17.58021 and 18.48903 g/min m^{-2} for CNT-TC and CNT-500 respectively, and it's almost doubled in comparing with FS evaporation flux.

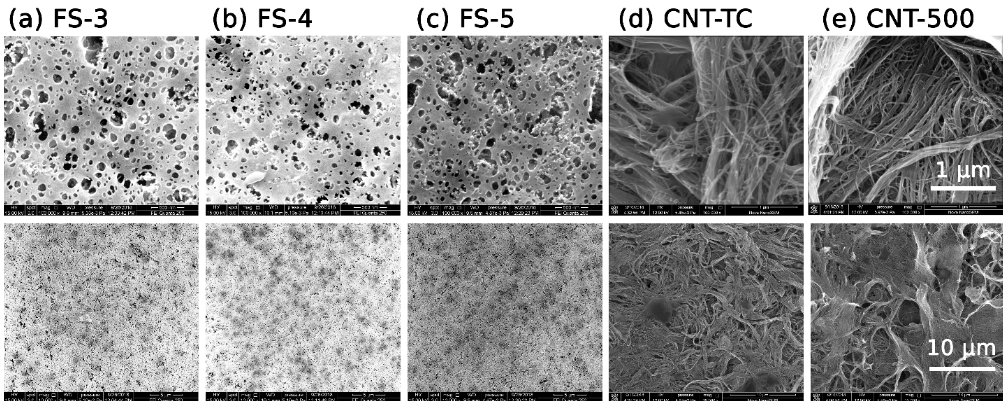

Fig. 4. SEM images of membrane samples prepared with nanoparticles.

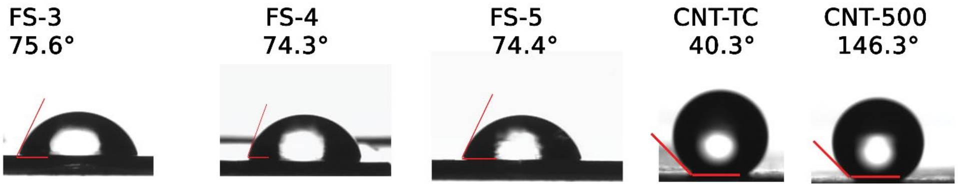

Fig. 5. Membranes' contact angle.

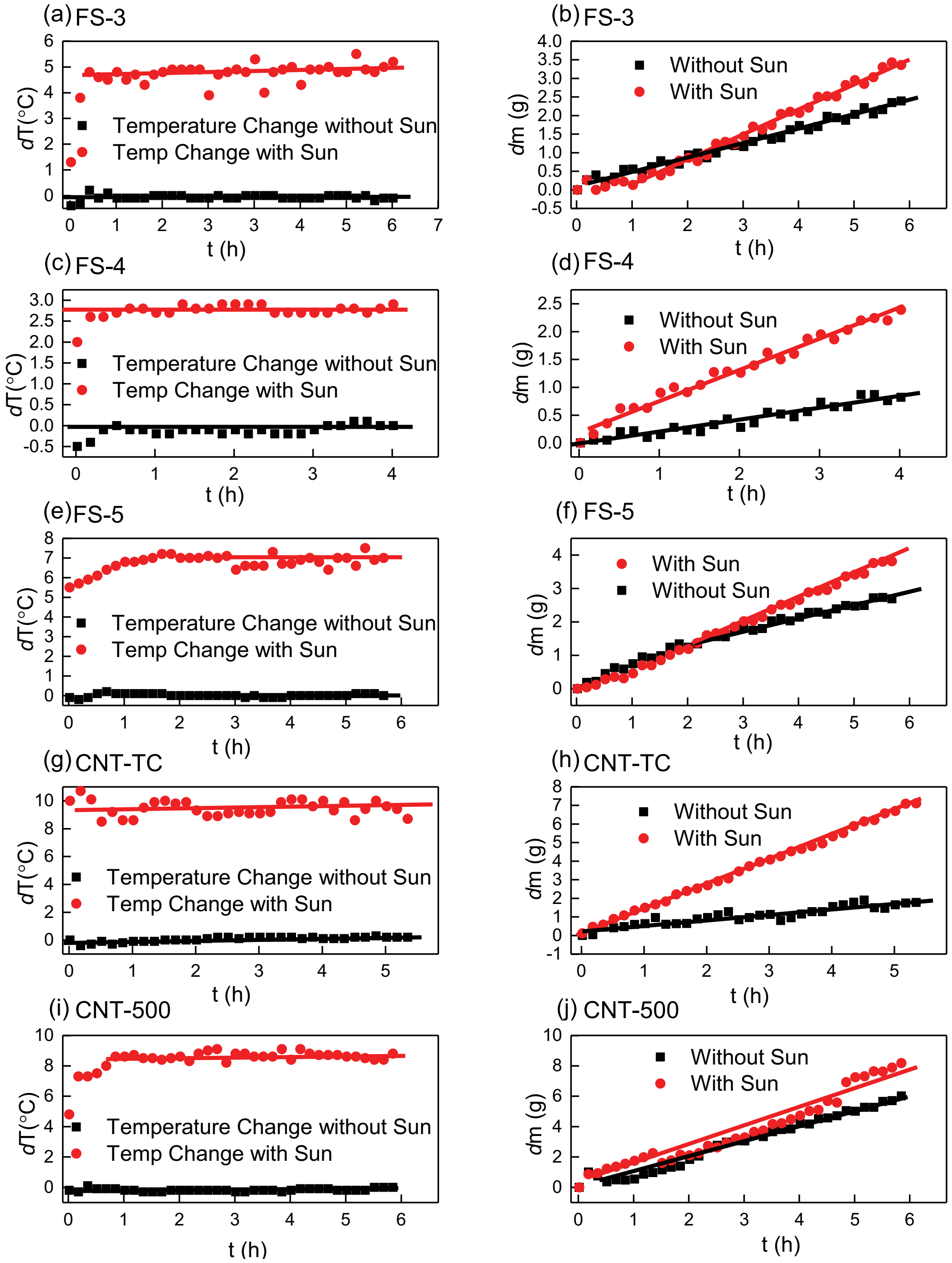

Fig. 6. Mass and temperature change of the membranes in this film evaporation test

Table 3
Porosity and MPS of Fabricated membrane

Membrane code	Mean pore size (MPS) µm	Porosity %
CNT-TC	0.1781	64.9
CNT-500	0.2234	71.6
FS-3	0.1279	81.1
FS-4	0.1186	83.1
FS-5	0.2267	74.6

3.2.1. Morphology

Fig. 4 shows the morphologies of CNT membrane, and its structure different than FS membranes. From the SEM picture, we can conclude that CNT-TC has smaller pores than CNT-500. This is because of using a different drying method. CNT-TC was dried using oven while CNT-500 dried using freezer.

3.2.2. Porosity and wettability

CNT-500 is more porous membrane than CNT-TC with MPS 0.2234 µm and 0.1781 µm, respectively. And both are super hydrophobic membranes which are favorable for thin film evaporation as shown in Fig. 5.

Even the evaporation flux was better in the bigger pore size membrane for CNT membranes we cannot give a conclusion in effect of pore size in evaporation flux. Since, more membranes with different pore sizes need to be investigated and tested.

4. Conclusion

Through a study of FS and CNT nanoparticles in thin film evaporation, it has been shown that CNT is an effective nanoparticle to obtain higher vapor flux in thin film evaporation that incorporated with solar simulator. One of the reasons is CNT has high ability to absorb light and converted it to thermal energy. The results show that there is an effect of pore size in steam generation via nanoporous membrane and it is still in progress and under investigation to end up with clear conclusion. And the same for thermal conductivity analysis, adding more semi conductive nanoparticle will increase the ability of converting light to thermal energy and thermal conductivity as well. The tradeoff between porosity and thermal conductivity of the membrane requires a deep study experimentally and theoretically.

References

Gewin, V., Industry lured by the gains of going green, Nature 436 (2005) 173.

Gleick, P.H., Water resources, in: Schneider, S.H., (Ed.) Encycl. Clim. Weather, 2, Oxford University Press, New York, USA 1996, pp. 817–823.

Peng, G., et al., "Low-cost high-efficiency solar steam generator by combining thin film evaporation and heat localization: Both experimental and theoretical study," Appl. Therm. Eng., vol. 143, no. August, pp. 1079–1084, 2018.

Plawsky, J. L., Fedorov, A. G., Garimella, S. V., Ma, H. B., Maroo, S. C., Chen, L., & Nam, Y. (2014). Nano-and microstructures for thin-film evaporation-A review. Nanoscale and Microscale Thermophysical Engineering, 18(3), 251–269. DOI: 10.1080/15567265.2013.878419.

Ni, G., "Solar steam generation by heat localization Solar steam generation by heat localization," Nat. Commun., vol. 5, no. August, pp. 1–7, 2014.

Neumann, O. et al. Solar vapor generation enabled by nanoparticles. ACS Nano 7, 42–49 (2012).

Wu, C.L., Lin, H.C., Hsu, J.S., Yip, M.C., Fang, W. Static and dynamic mechanical properties of polydimethylsiloxane/carbon nanotube nanocomposites. Thin Solid Films 2009, 517, 4895–4901.

Suzuki, N., Kamachi, Y., Takai, K., Kiba, S., Sakka, Y., Miyamoto, N., Yamauchi, Y. Effective use of mesoporous silica filler: Comparative study on thermal stability and transparency of silicone rubbers loaded with various kinds of silica particles. Eur. J. Inorg. Chem. 2014, 2014, 2773–2778.

Mavukkandy, M. O., Bilad, M. R., Kujawa, J., Al-Gharabli, S., Arafat, H. A., "On the effect of fumed silica particles on the structure, properties and application of PVDF membranes," Sep. Purif. Technol., vol. 187, pp. 365–373, 2017.